



## Search for Charged Higgs Bosons with the ATLAS Detector

Liron Barak on behalf of the ATLAS Collaboration

*Weizmann Institute of Science*

---

### Abstract

The search for charged Higgs is an integral part of the Higgs boson studies at the LHC. The discovery of such a particle would be a clear evidence of physics beyond the standard model. Several non-minimal Higgs scenarios, e.g. Two Higgs Doublet Models (2HDM), predict the existence of charged Higgs bosons. In this article we review searches for charged Higgs boson produced in three modes; in top decay, in association with a top quark, or in neutral Higgs boson decay. Results are based on data collected by the ATLAS experiment in 2011 and 2012 at the LHC. No significant deviation from the standard model background expectation is found in any of the searches presented and corresponding constraints on physics beyond the Standard Model are obtained.

*Keywords:* ATLAS, Beyond Standard Model, Two Higgs Doublet Models, Charged Higgs

---

### 1. Introduction

The BEH mechanism was suggested 50 years ago in order to explain how elementary particles acquire mass within the Standard Model. The Higgs boson, which clearly confirms this mechanism, was discovered in July 2012. This discovery marked the beginning of an exciting experimental period in which the Higgs properties predicted by the SM are precisely measured and searches for properties beyond the SM are performed. Searches for beyond-the-SM (BSM) Higgs bosons are highly motivate, since they provide direct information on a possibly extended scalar sector. A large number of searches for BSM Higgs bosons have been performed by the ATLAS collaboration at the LHC, using collision data at a center-of-mass energy of 7 TeV (2011) and 8 TeV (2012). In the following, an overview of recent results of searches for charged Higgs are presented.

### 2. Charged Higgs Searches

Despite of its great success in describing the world of elementary particles, the SM does not explain all known phenomena; Neutrino masses, Dark matter and Baryon asymmetry are of the common examples. This indicates

that the SM is not the complete theory of nature and suggests that it has to be extended. One possibility is an extended Higgs sector which, similarly to the three generation of leptons and quarks, consists of more than a single Higgs scalar. The most significant constraint on such an extended Higgs sector derived from the observational fact that  $\rho \equiv m_W/(m_Z \cos \theta_W) \approx 1$ . This property is often violated when general extended Higgs sectors are considered and thus requires a certain level of fine tuned parameters to satisfy the experimental constraints. It is conserved at tree level in extensions employing SU(2) doublets or singlet, out of which the Two Higgs Doublet Models (2HDM) and particularly its CP conserving version is the most studied one.

After electroweak symmetry breaking, 2HDM predicts five physical scalar particles: two CP-even bosons,  $h$  and  $H$  (defined such that  $m_h < m_H$ ), one CP-odd particle,  $A$ , and two charged scalar particles,  $H^\pm$ . Different searches for charged Higgs have been performed. These searches have been designed and optimized to comply with the different signatures arising from the different production mechanisms and decay modes of the charged Higgs.

At the LHC and in the so-called type-II 2HDM,

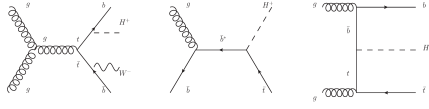


Figure 1: Leading-order Feynmann diagrams of the dominant production modes of charged Higgs bosons at masses below (left) and above (center and right) the top-quark mass.

which is also the Higgs sector of the Minimal Supersymmetric Standard Model (MSSM), two main production modes are considered depending on the mass of the charged Higgs; For mass below the top quark mass ( $m_{H^+} < m_{\text{top}}$ ) we consider the production through the top quark decay  $t \rightarrow bH^+$  (Fig. 1 - left diagram), at the LHC the top pair production is the main top resource. For masses greater than  $m_{\text{top}}$ ,  $H^+$  is mostly produced at the LHC in association with top quark. An additional  $b$  quark can also appear in the final state (Fig. 1 - center and right diagrams).

In the MSSM, the Higgs sector, as well as all decay channels, can be completely determined at tree level by one of the Higgs boson masses, here taken to be  $m_{H^+}$ , and  $\tan\beta$  - the ratio of the vacuum expectation values of the two Higgs doublets. For  $m_{H^+} < m_{\text{top}}$ , the decay  $H^+ \rightarrow \tau\nu$  is dominant for  $\tan\beta > 2$  and remains sizeable for  $1 < \tan\beta < 2$ . However, for low  $\tan\beta$  values and for types other than type-II in the CP conserved 2HDM,  $H^+ \rightarrow c\bar{s}$  is the dominant decay. For higher  $m_{H^+}$ ,  $H^+ \rightarrow t\bar{b}$  is the dominant decay. Nevertheless,  $H^+ \rightarrow \tau\nu$  is still significant, especially for large values of  $\tan\beta$ .

### 3. $H^+ \rightarrow c\bar{s}$

A search for light charged Higgs ( $m_{H^+} < m_{\text{top}}$ ) was conducted using  $4.7 \text{ fb}^{-1}$  of LHC data collected by the ATLAS detector at  $\sqrt{s} = 7 \text{ TeV}$ . The search was for light charged Higgs bosons produced in semi-leptonic  $t\bar{t}$  events where one of the top quarks decays via  $t \rightarrow H^+b$ , followed by  $H^+ \rightarrow c\bar{s}$  [1]. The other top quark decays to  $Wb$ , where the  $W$  boson further decays into a lepton ( $e/\mu$ ) and a neutrino. Consequently, the analysis strategy was identifying the typical kinematics of a signal events (using a kinematic fitter techniques) within a semi-leptonic  $t\bar{t}$  events. The SM backgrounds consist of  $t\bar{t}$ , single top quark,  $W$  and  $Z$  bosons with additional jets, diboson and QCD multi-jets. The analysis requires an isolated high  $P_T$  lepton ( $e/\mu$ ), 4 high  $P_T$  jets (two of them  $b$ -tagged), missing transverse energy ( $E_T^{\text{miss}}$ ) and the transverse mass  $m_T$  of the lepton and  $E_T^{\text{miss}}$  cut ( $m_T$  defined as  $2P_T^l E_T^{\text{miss}}(1 - \cos\Delta\phi)$ , where  $\Delta\phi$  is the azimuthal angle between the lepton and the missing trans-

verse momentum). After applying these selections, a  $\chi^2$ -based kinematic fit is applied with the goal of finding a second mass peak in the di-jet distribution consistent with  $H^+ \rightarrow c\bar{s}$  events. In the kinematic fitter, the lepton,  $E_T^{\text{miss}}$  (assumed to be from the neutrino), and four jets are assigned to the decay particles from the  $t\bar{t}$  system. The fitter also constrains the invariant mass of the two systems ( $b\ell\nu$ ,  $bjj$ ) to be within  $\gamma_t = 1.5 \text{ GeV}$  of the top-quark mass  $172.5 \text{ GeV}$ . The jet combination with the minimal  $\chi^2$  value,  $\chi_{\text{min}}^2$ , is selected as the best assignment. Events with  $\chi_{\text{min}}^2 > 10$  are rejected to remove poorly reconstructed  $t\bar{t}$  events. The  $\chi_{\text{min}}^2$  distribution for selected events in the data agrees well with the SM expectations. The fit results in a  $12 \text{ GeV}$  di-jet mass resolution regardless of the mass of the boson studied. This is 20-30% improvement compared to the resolution obtained when the same jets are used with their original transverse momentum measurements.

Most of the SM background sources (SM  $t\bar{t}$ , single top quark,  $Z$  boson with additional jets and diboson) were estimated by using Monte-Carlo (MC) simulation. The QCD multi-jet background is estimated using a data-driven method that employs a likelihood fit to the  $E_T^{\text{miss}}$  distribution in the data, using a template for the multi-jet background and templates from MC simulations for all other processes. The rate of  $W$ +jets events is estimated by a data-driven method that uses the observed difference in the number of  $W^+$  and  $W^-$  bosons in the data and the charge asymmetry  $(W^+ - W^-)/(W^+ + W^-)$ , which is calculated to a good precision by the MC simulation of  $W$ +jets events. The heavy flavour fraction of the  $W$ +jets MC simulation is calibrated using  $W + 1 \text{ jet}$  or  $W + 2 \text{ jets}$  events in the data.

The data is found to be in good agreement with the distribution of the di-jet mass expected from SM processes (see Fig. 2). The fractional uncertainty on the signal-plus-background model is comparable to the background only model. 95% Confidence level (CL) upper limits on the branching ratio  $B(t \rightarrow H^+b)$  are extracted as a function of the charged Higgs mass. It varies between 5% and 1% for  $H^+$  masses between  $90 \text{ GeV}$  and  $150 \text{ GeV}$ , assuming  $B(H^+ \rightarrow c\bar{s}) = 100\%$ , as can be seen in Fig. 3.

### 4. $H^+ \rightarrow \tau\nu$

A search for the light and heavy charged Higgs boson using the  $\tau$  + jets channel with a hadronically decaying  $\tau$  lepton in the final state [2] was performed using  $19.5 \text{ fb}^{-1}$  of proton-proton collision data collected by the ATLAS detector at  $\sqrt{s} = 8 \text{ TeV}$ . Two production modes,

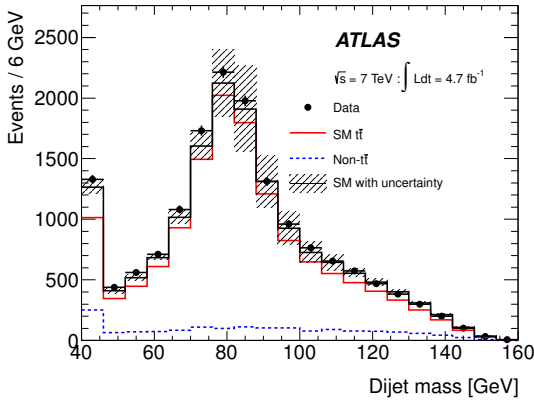


Figure 2: The dijet mass distribution measured in the data and the expectation from the SM ( $Br = 0$ ). The error bars represent the statistical uncertainty on the data. The uncertainty shown on the background estimate is the combination in quadrature of the  $\pm 1\sigma$  systematic uncertainties, accounting for the constraint from the profile likelihood fit. The first and last bins contain the underflow and overflow events respectively.

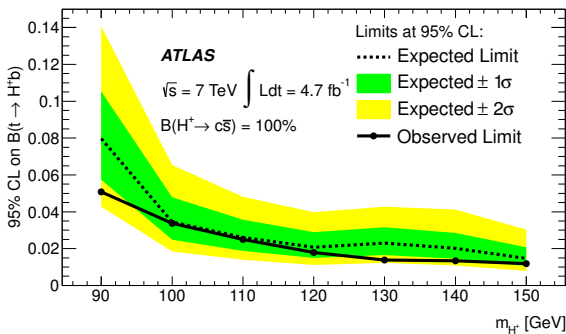


Figure 3: The extracted 95% CL upper limits on  $B(t \rightarrow H^+ b)$ , assuming that  $B(H^+ \rightarrow c\bar{s}) = 100\%$ , are shown for charged Higgs mass in the range 90–150 GeV. The limits shown are calculated using the  $CL_s$  limit-setting procedure.

depending on the  $H^\pm$  mass, were studied;  $t\bar{t} \rightarrow H^+ b W b$  for light charged Higgs bosons ( $m_{H^\pm} < m_{top}$ ) and associated production of  $tH^+$  for heavy charged Higgs bosons; the dominant production modes in the two scenarios. A  $\tau_{had-vis} + E_T^{miss}$  trigger, dedicated specifically for this analysis, was used. The trigger requirement is followed by selecting events with at least 4 (3) high  $P_T$  jets (at least one of them b-tagged), exactly one high  $P_T$  hadronically decaying  $\tau$  (with no other electron, muon or tau), missing transverse energy ( $E_T^{miss}$ ) and a requirement placed on the quantity  $\frac{E_T^{miss}}{0.5 \cdot \sqrt{\sum p_T^{PVirk}}} > 13$  (12)  $GeV^{1/2}$  in the light (heavy)  $H^+$  search. Here  $p_T^{PVirk}$  is the transverse momentum of a track originating from the primary vertex and the sum is taken over all tracks from the PV. The final discriminating variable is the  $\tau_{had-vis} + E_T^{miss}$  transverse mass, defined as  $2P_T^l E_T^{miss} (1 - \cos \Delta\phi)$ , where  $\Delta\phi$  is the azimuthal angle between the lepton and the missing transverse momentum.

Backgrounds to the search for charged Higgs bosons in the  $\tau$  + jets final state is categorized according to the origin of the hadronically decaying  $\tau$  candidate in the event. Three categories are considered: events with muon or electron misidentified as hadronic tau, background with real hadronic tau and background from events with jet misidentified as hadronic tau. Background sources where an electron or a muon are misidentified as a  $\tau$  and backgrounds with true hadronic  $\tau$  are estimated from MC simulation corrected to account for known data-MC discrepancies. In particular, events with real hadronic  $\tau$  are modified by scale factors that correct the efficiency of the  $\tau_{had-vis}$  identification algorithm in simulation to that measured in data. Scale factors are also applied to correct the simulated efficiency of the electron veto algorithm (used to suppress background from electron misidentified as  $\tau$ ) to that measured in data. Background arising from both gluon-initiated and quark-initiated jets is assessed using a data-driven method that applies weights calculated from identification and misidentification efficiencies to data events.

As can be seen in Fig. 4, for both the light and heavy charged Higgs boson, the data agrees well with the SM expectations. In absence of evidence for charged Higgs boson, 95% confidence level (CL) upper limits are set. These upper limits are set on the branching fraction  $B(t \rightarrow H^+ b)$  for the light charged Higgs boson scenario and on the production cross section  $\sigma(pp \rightarrow t(b)H^+)$  for the heavy charged Higgs boson scenario, assuming  $B(H^+ \rightarrow \tau^+ \nu) = 100\%$  in both scenarios (Fig. 5). For  $m_{H^\pm}$  in the range 90–160 GeV, upper limits are set in a

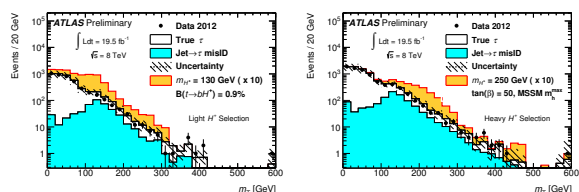


Figure 4: The observed data and background predictions after applying the nominal selection in the (left) light charged Higgs boson search and in the (right) heavy charged Higgs boson search. In the distributions of the light  $H^+$  signal selection, a signal of  $m_{H^+} = 130$  GeV and  $B(t \rightarrow H^+ b) = 0.9\%$  is included. In the heavy  $H^+$  signal selection, a signal of  $m_{H^+} = 250$  GeV and  $\tan\beta = 50$  with the cross section and  $B(H^+ \rightarrow \tau\nu)$  of the MSSM  $m_h^{max}$  scenario is included. All signal contributions are scaled up by a factor of 10. The last bin of each  $m_t$  distribution includes overflow. The uncertainty band shows the pre-fit systematic uncertainties, added in quadrature.

range of  $B(t \rightarrow H^+ b) = 0.24 - 2.1\%$ . For  $m_{H^+}$  in the range 180-600 GeV, upper limits are set on the production cross section of the charged Higgs boson in a range of 0.017 – 0.90 pb.

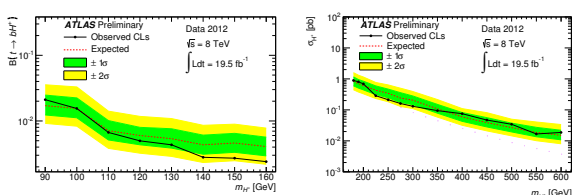


Figure 5: The expected and observed 95% CL upper limits in the light charged Higgs boson (left) scenario and in the heavy charged Higgs boson (right) scenario, assuming  $B(H^+ \rightarrow \tau\nu) = 1$ .

The exclusion limits on the light and heavy  $H^+$  are also interpreted in terms of the MSSM  $m_h^{max}$  scenario with  $\mu = 200$  GeV, shown in Fig. 6. This corresponds to an exclusion of  $\tan\beta > 1$  in the  $\tan\beta$ - $m_{H^+}$  parameter space for  $m_{H^+}$  in the range 100-140 GeV. Only small regions of parameter space for  $m_{H^+}$  in the range 90-100 GeV and 140-160 GeV are not excluded. For heavy charged Higgs bosons with  $m_{H^+} > m_{top}$ , values of  $\tan\beta$  in the range 47 and 63 are excluded for  $m_{H^+}$  in the range 200-300 GeV.

## 5. Charged Higgs in 2HDM Cascade

The existence of an extended scalar sector with more than one Higgs bosons allows for cascade decays in which heavier Higgs bosons (produced via gluon-gluon fusion), initiate a cascade decay to charged Higgs,  $H^\pm$ , which further decays to a light neutral Higgs boson,  $h$ . Such a cascade contains three resonances and results in

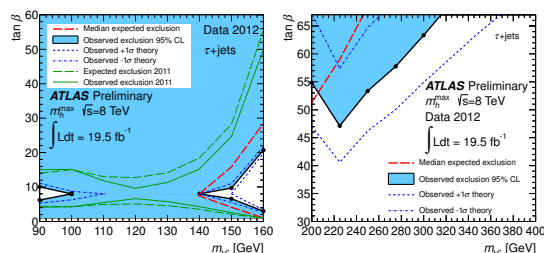


Figure 6: Interpretation of the limits on the branching fractions of the light  $H^+$  (left) and the production cross section of the heavy  $H^+$  (right), in the context of the MSSM  $m_h^{max}$  scenario with  $\mu = 200$  GeV. For comparison, the 2011 limits are overlaid in green for the light  $H^+$  limit interpretation.

a  $W$ -boson pair and a bottom-antibottom quark pair in the final state (see Fig. 7). In this context, a Higgs boson cascade has been looked for using  $20.3 \text{ fb}^{-1}$  of  $\sqrt{s} = 8$  TeV proton-proton collision data collected by the ATLAS detector [3]. Rather than assuming a particular

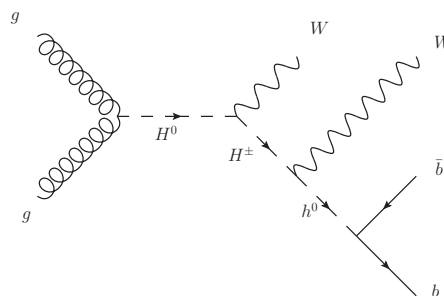


Figure 7: Diagram of the Higgs-boson cascade  $gg \rightarrow H^0 \rightarrow W^\mp H^\pm \rightarrow W^\mp W^\pm h^0 \rightarrow W^\mp W^\pm b\bar{b}$ .

theoretical model, this analysis follows the so-called “simplified model” approach by searching for a specific multi-Higgs-boson cascade topology. This analysis looks for multiple simultaneous resonances,  $b\bar{b}$ ,  $b\bar{b}W$  and  $b\bar{b}WW$ , in  $t\bar{t}$ -like ( $b\bar{b}WW$ ) events. Fixing the mass of the lightest Higgs at 125 GeV, leaves the mass of the heavy and charged Higgses as the only two free parameters in the model. The main background in this search is the SM  $t\bar{t}$  pair production. The semi-leptonic channel (where one  $W$  decays leptonically and the second hadronically) was used for optimal sensitivity. Event selection is based on the signature of  $t\bar{t}$  event (share the same final state), assuming that one of the  $W$ -bosons decays leptonically (either to electron or muon and corresponding neutrino). The typical  $t\bar{t}$  event has a high  $-p_T$  lepton, at least four jets, two of which are  $b$ -tagged jets, large  $E_T^{miss}$  and transverse  $W$  mass (to reduce the

contamination from fake leptons).

Simple reconstruction techniques were used to reconstruct the mass of the  $h$ ,  $H^\pm$  and  $H$ ; the  $h$  mass was estimated as the invariant mass of the 2  $b$ -tagged jets. The mass of the Hadronic  $W$  was estimated as the invariant mass of the remaining jets with the di-jet mass closest to 80.4 GeV. The 2HDM cascade and a typical SM  $t\bar{b}$  cascade differ in many kinematic variables such as the directions and masses of the reconstructed resonances. The best sensitivity was obtained using multivariate (MVA) techniques exploiting the discriminating power of all the kinematic variables. Separate MVA was used for each signal mass point in order to take into account variations in the kinematic distributions between the different mass points.

The observed yields are found to be consistent with the SM background expectations, within uncertainties. The MVA outputs for two example signal mass points are shown in Fig. 8.

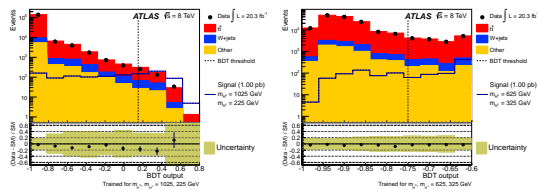


Figure 8: Distributions of the MVA output in the signal regions for two example signal mass points,  $m(H^0)$ ,  $m(H^{+-}) = 1025, 225$  GeV (left),  $m(H^0)$ ,  $m(H^{+-}) = 625, 325$  GeV (right). Signal histograms have been scaled to a production cross section of 1 pb. BDT thresholds are shown as dashed lines for each mass point. The background model is shown as the coloured stacked histogram. The last bin contains the overflow events

In the absence of signal, cross-sectional limits are set on generic resonance cascades decays (Fig. 9).

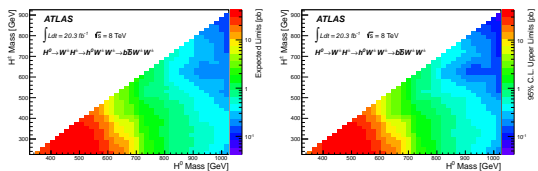


Figure 9: The expected (left) and observed (right) 95% C.L. upper limits on the cross section for  $gg \rightarrow H^0 \rightarrow WH^\pm \rightarrow WW h \rightarrow WW bb$  as a function of  $m(H^0)$  and  $m(H^\pm)$ .

By following a simplified model approach, such limits may be re-interpreted in the context of many new untested models. For instance, limits on the heavy neutral Higgs were extracted in the context of 2HDM.

## 6. Conclusions

The search for beyond SM Higgs bosons is highly motivated and provide with a rich environment to study different signatures. Charged Higgs bosons searches have been performed by the ATLAS collaboration using fermionic and bosonic couplings both in the production and the decay modes. Light charged Higgs produced in top decays was searched for in two decay channels; the decay to  $c\bar{s}$  (at 7 TeV) and the decay to  $\tau\nu$  (at 8 TeV). Heavy charged Higgs was searched in the  $\tau\nu$  channel. Since no deviations from the SM expectations was observed, upper limits are set; on the branching fraction  $B(t \rightarrow H^\pm b)$  in the light charged Higgs boson scenario and on the production cross section  $\sigma(pp \rightarrow t(b)H^\pm)$  in the heavy charged Higgs boson scenario, with  $B(H^\pm \rightarrow \tau^\pm\nu) = 100\%$ . Using the  $\tau\nu$  decay, the MSSM  $m_{max}^h$  scenario was constrained. In the 2HDM cascade, the charged Higgs is produced and decay to bosons (W and Higgs). In that search (at 8 TeV), cross-sectional limits are set. With more data expected to be delivered by the LHC the Charged Higgs frontier will definitely be further pursued.

## References

- [1] The ATLAS collaboration, Eur. Phys. J. C **73**, 2465 (2013) [arXiv:1302.3694 [hep-ex]].
- [2] The ATLAS collaboration, ATLAS-CONF-2013-090, ATLAS-COM-CONF-2013-107.
- [3] The ATLAS collaboration, Phys. Rev. D **89**, no. 3, 032002 (2014) [arXiv:1312.1956 [hep-ex]].